MOLECULAR REACTION DYNAMICS

Hilary Term 2023

4 Lectures

Prof Mark Brouard

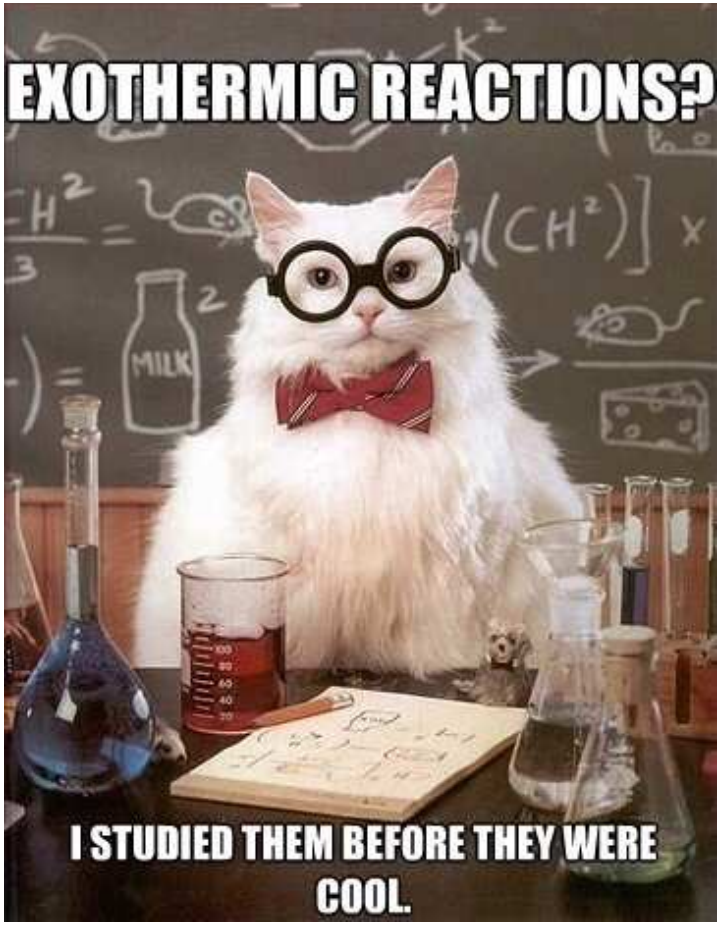

MOLECULAR REACTION DYNAMICS

Hilary Term 2023

4 Lectures

Prof Mark Brouard

Aims: *Understanding, predicting, and controlling chemical reactivity.*

What is the nature of the forces at play in chemical reactions?

What is the nature of the potential energy surface(s)?

Outline plan:

1. *Introduction*
2. *Potential energy surfaces*
3. *Experimental techniques - initial states*
4. *Experimental techniques - final states*
5. **Elastic and Inelastic scattering**
6. **Reactive scattering**
7. **Controlling reagents and characterizing products**
8. **Probing the transition state.**

Types of encounter

Cross-sections can be defined and measured for many different types of collision

We will consider three categories of collisions (see Professor Vallance's lectures):

(a) Elastic scattering: conserves kinetic energy, leads to a change in direction.

(b) Inelastic scattering: leads to a change in internal energy of the colliders.

(c) Reactive scattering: leads to a rearrangement of bonds.

Apart from today's lecture we will focus on *reactive collisions*.

The **motivation** is to understand the forces operating in molecular collisions.

Elastic scattering

Simple measurement of a cross-section

Example of a 'beam-gas' experiment.

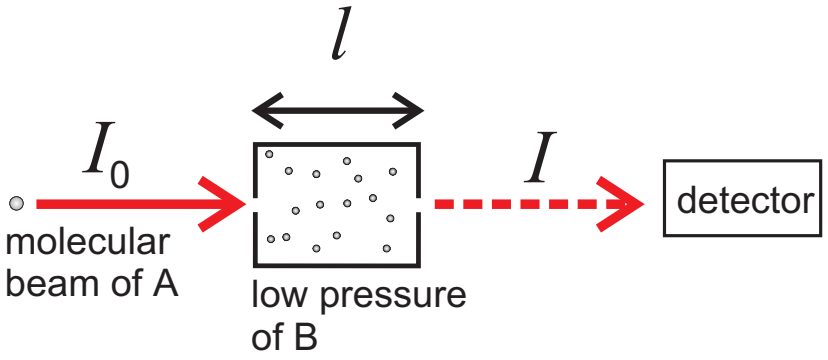

When molecules of A collide with B they are deflected. This leads to attenuation of the molecular beam of A.

Use the equivalent of *Beer-Lambert law* for light

$$I = I_0 \, \mathrm{e}^{-\sigma c_\mathrm{B} l}$$

σ — the **elastic scattering cross-section**,

c_B — the concentration of B, and

l — the path length of B through which A passes.

Elastic scattering cross-section: Glory scattering

Striking quantum effects are observed for atom-atom scattering (*e.g.*, K + Rg).

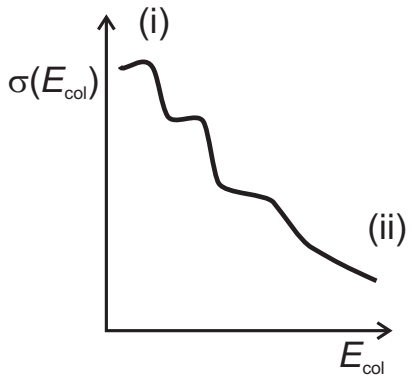

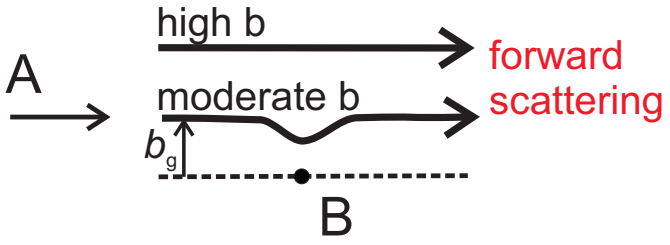

Glory oscillations arise from quantum mechanical interference between two pathways (two de Broglie waves) leading to scattering in the *forward* direction (the original direction of motion of A).

What do we learn about the potential energy curve (or the forces operating during the collision)?

The frequency of the oscillations varies with collision energy because the phase difference between the two pathways varies with velocity.

(i) High collision energies probe the repulsive part of the potential

(ii) Low collision energies probe the attractive part of the potential

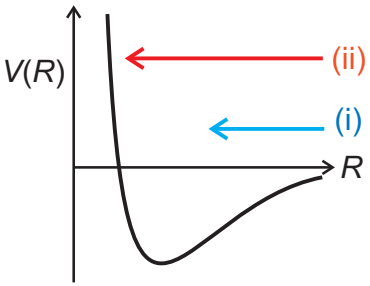

Crossed beam experiment

Crossed molecular beam measurements provide the **angular distribution** of the products.

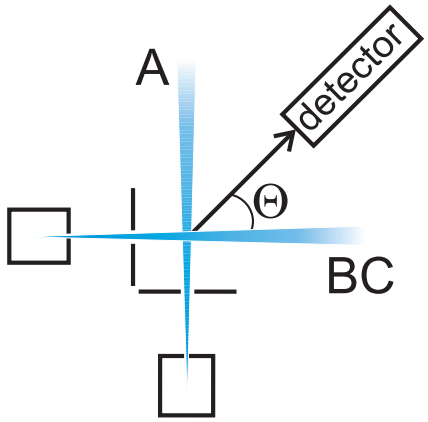

As you have seen already from previous lectures, data are obtained in the laboratory (left)....

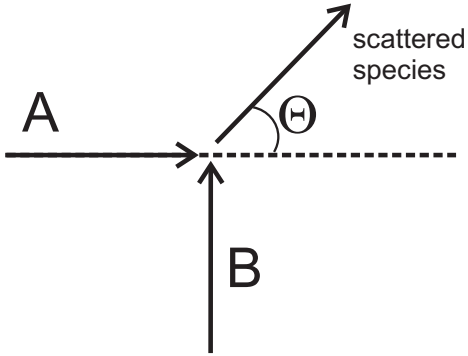

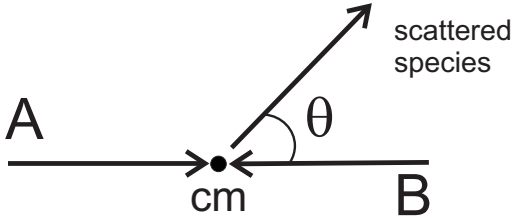

....but are usually plotted with respect to the centre-of-mass (cm) (right).

We need to transform the data from the laboratory (lab) frame to the centre-of-mass (cm) frame. In the cm frame (right hand figure) the centre-of-mass is stationary.

The differential cross-section

The dependence of the cross-section on **scattering angle** is quantified by the **differential cross-section**

$$\frac{\mathrm{d}\sigma}{\mathrm{d}\omega}$$

where $\mathrm{d}\omega$ represents the cm solid angle volume element $\sin\theta \mathrm{d}\theta\mathrm{d}\phi$.

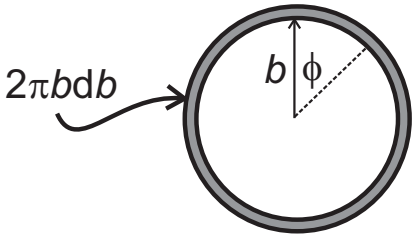

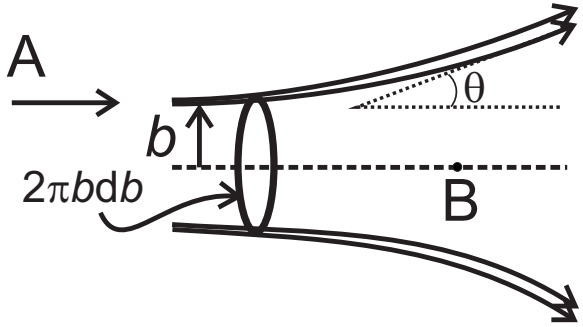

The integral of the differential cross-section (DCS) over scattering angles gives the total or **integral cross-section**

$$\sigma = \int_0^{2\pi} \int_0^{\pi} \frac{\mathrm{d}\sigma}{\mathrm{d}\omega} \sin\theta \mathrm{d}\theta\mathrm{d}\phi$$

The dimensions of the DCS are of area per steradian.

The angular distribution of the scattered products

The **angular distribution** of the products can be expressed as

$$P(\theta, \phi) = \frac{1}{\sigma} \frac{\mathrm{d}\sigma}{\mathrm{d}\omega},$$

where $P(\theta, \phi)\mathrm{d}\omega$ **is the probability of finding products scattered into solid angles between** ω **and** $\omega + \mathrm{d}\omega$.

Recall that classically the integral cross-section can be obtained from the equation

$$\sigma = \int_0^{b_{\mathrm{max}}} P(b) 2\pi b \mathrm{d}b,$$

where $P(b)$ is the *opacity function*, which quantifies the collision (or reaction) probability as a function of impact parameter, b.

Due to the 'dart-board' averaging over impact parameter (as implied by the above equation and as illustrated on the previous slide), and provided the reactants are not oriented, **the differential cross-section and angular distribution are independent of the azimuthal angle,** ϕ. We can therefore write:

$$P(\theta) = \int_0^{2\pi} P(\theta, \phi) \mathrm{d}\phi = \frac{2\pi}{\sigma} \frac{\mathrm{d}\sigma}{\mathrm{d}\omega}$$

Rainbows in elastic scattering of atoms

Again, we expect to see quantum mechanical **interference**.

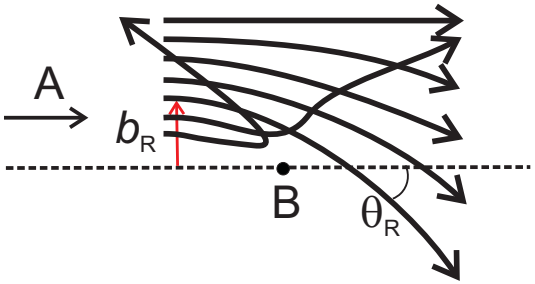

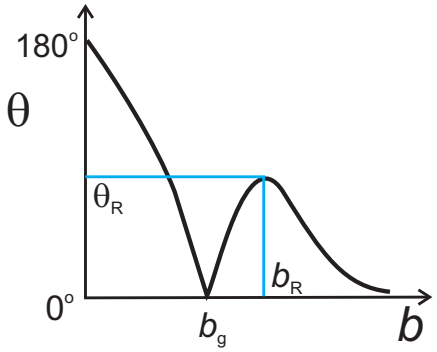

At the **rainbow angle** the gradient $\mathrm{d}\theta/\mathrm{d}b = 0$. Classically one finds a discontinuity in differential cross-section at θ_R.

For $\theta < \theta_R$, three values of b lead to deflection through the same scattering angle. In quantum mechanics, this leads to interference known as supernumerary rainbows.

The features in $\frac{\mathrm{d}\sigma}{\mathrm{d}\omega}$ are directly related to the nature of the potential energy curve.

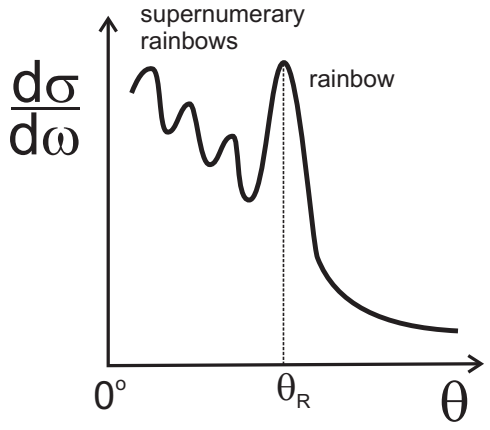

θ_R is sensitive to the well depth in potential.

The supernumerary rainbows provide information about the range and shape of the potential near the minimum.

Inelastic scattering: collisional energy transfer

Inelastic collisions lead to a transfer of energy from one form to another, or between one molecule and another:

Translation **Rotation** **Vibration** **Electronic**

For example:

Translation $\rightarrow$ *Vibration* (T $\rightarrow$ V)

$$\mathrm{Ar} + \mathrm{CO}(v=0) \longrightarrow \mathrm{Ar} + \mathrm{CO}(v=1)$$

Vibration $\rightarrow$ *Vibration* (V $\rightarrow$ V)

$$\mathrm{N_2}(v=0) + \mathrm{CO}(v=1) \longrightarrow \mathrm{N_2}(v=1) + \mathrm{CO}(v=0)$$

Huge literature on these types of process.

General ideas for T, R, V transfer

T $\rightarrow$ V,R	Probability $\uparrow$ as energy converted into vibration or rotation $\downarrow$.
T $\rightarrow$ R	Usually much more efficient than T $\rightarrow$ V
V $\rightarrow$ V	Probability $\uparrow$ as energy converted into translation or rotation $\downarrow$ (*i.e.* as the *mismatch* between the vibrational levels $\downarrow$).

Controlling factors?

(i) **LOW** efficiency processes	*e.g.*, T $\rightarrow$ V Small cross-sections Usually involve small b (head-on) collisions Controlled by short range repulsion
(ii) **HIGH** efficiency processes	*e.g.*, T $\rightarrow$ R or resonant V $\rightarrow$ V Large cross-sections Usually involve a large range of b Controlled by long-range attraction (*e.g.*, dipole-dipole, etc.)

Scattering experiment

Crossed molecular beam experiment (such that H_2 is initially cooled into its lowest rotational and vibrational states)

$$Li^+ + H_2(v = 0, j = 0, 1) \longrightarrow Li^+ + H_2(v', j')$$

Observe the change in velocity of Li^+ as a function of scattering angle (using time-of-flight mass spectrometry).

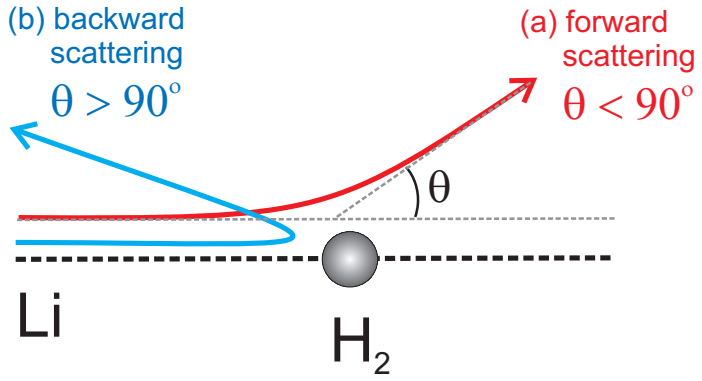

(a) Forward: Small KE loss in Li^+
corresponds to excitation of $H_2(v = 0, j = 1) \rightarrow H_2(v' = 0, j' = 3)$

Large b Large cross-section.

(b) Backward: KE loss much larger
corresponds to excitation of $H_2(v = 0, j = 1) \rightarrow H_2(v' = 1, 2, 3, j')$

Small b Small cross-section

Ne + CO($v = 0$, low j) $\longrightarrow$ Ne + CO($v' = 0, j'$)

CO(v', j') probed state-selectively using REMPI (see CV lectures).

Ions are then detected using the velocity map ion-imaging technique (see CV lectures).

'Newton Diagram'

Forward scattering

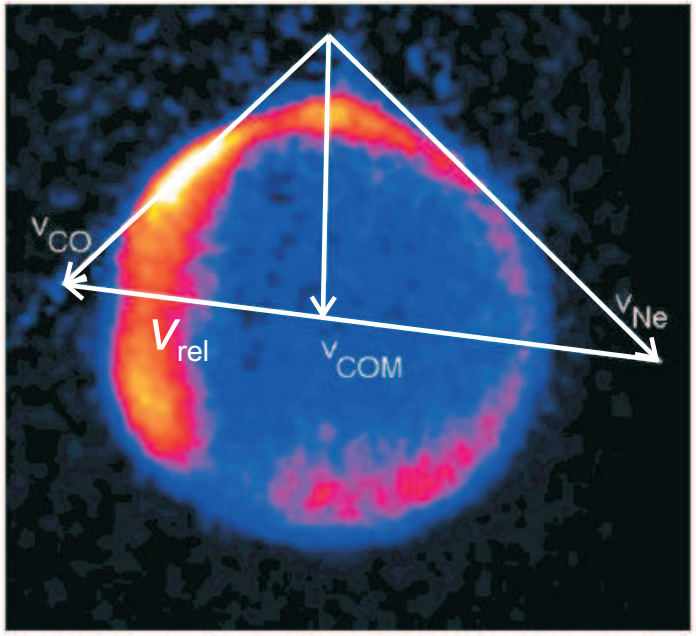

. Raw data for $j_f = 8$ with corresponding Newton diagram. The intersection near the top of the image gives the laboratory frame origin.

Backward scattering

The Newton (vector) diagram is superimposed on the ion image for CO products born in the $j' = 8$ rotational state.

D.W. Chandler *et al.*, *J. Phys. Chem. A*, **106**, 1144, (2002)

Dependence on CO($v' = 0, j'$)

Rings get smaller as j' increases, reflecting the lower velocity of internally excited CO.

This is simply due to energy conservation.

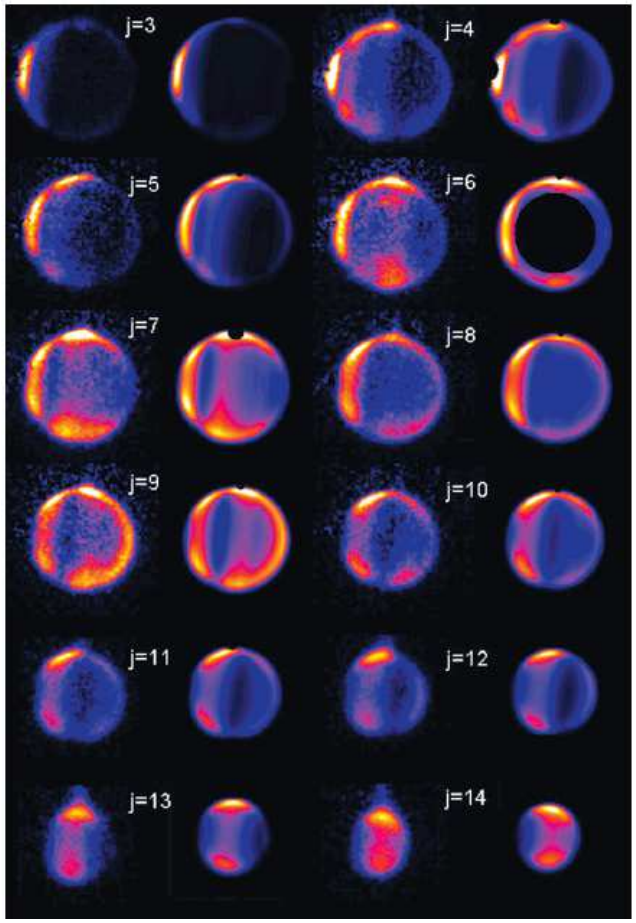

Intensity around the ring reflects the angular distribution.

The angular distribution must change as j' increases (see next slide).

D.W. Chandler *et al.*, *J. Phys. Chem. A*, **106**, 1144, (2002)

Ne + CO($v = 0$, low j) $\longrightarrow$ Ne + CO(v', j')

Differential cross-sections

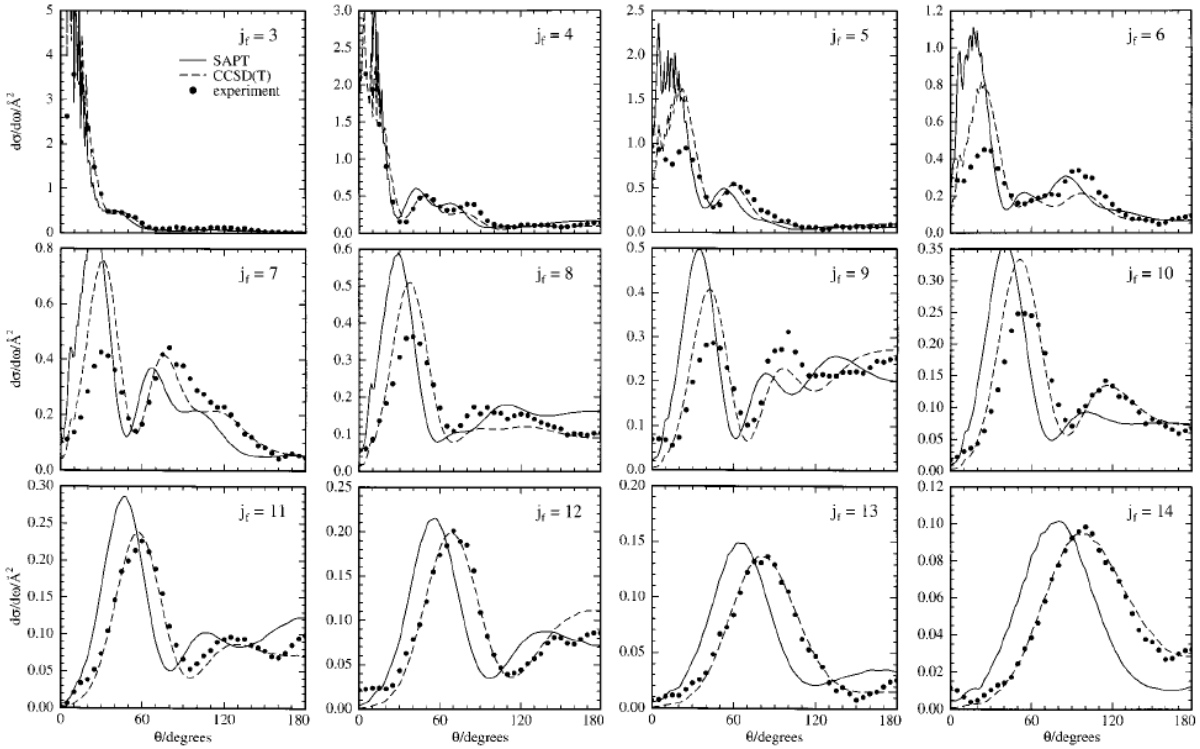

Figure 3. Experimental and calculated state-to-state differential cross sections.

Angular distribution changes from forward to backward scattering as the CO rotational level j' increases.

Oscillations are a manifestation of *quantum mechanical interference* similar to that described for atom-atom scattering.

D.W. Chandler *et al.*, *J. Phys. Chem. A*, **106**, 1144, (2002)

2. Angular distributions in reactive scattering

Molecular beam scattering

One of the molecular beams is usually chopped or pulsed to provide timing for time-of-flight MS measurement, from which product lab velocity is calculated (see CV lectures).

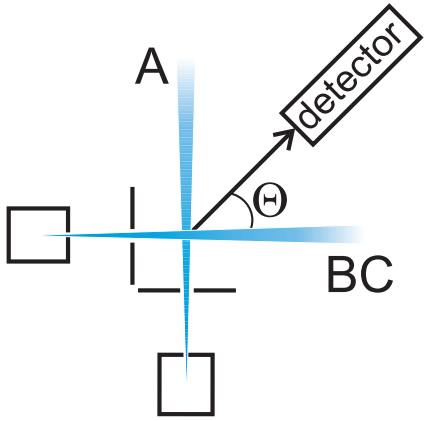

Detectors

- *Hot wire ionization*

  $$\text{M or MX} \rightarrow \text{Ions} \rightarrow \text{current}$$

  Good angular resolution, but relatively poor speed (energy) resolution

  $$K + I_2 \longrightarrow KI + I$$

- *Electron impact ionization coupled with mass spectrometry*

  Universal detection method, but rarely has sensitivity to allow product quantum state resolution. For an exception, see the reaction (discussed below)

  $$F + H_2 \longrightarrow HF + H$$

- *Spectroscopic methods*

  Usually based on laser ionization methods, and have high energy resolution. Only recently have they been applied to reactions in crossed molecular beam experiments due to low sensitivity

  $$H + HD \longrightarrow H_2 + D$$

Stripping and harpoon mechanisms

Early example

$$K + I_2 \longrightarrow KI + I$$

Plot data in the form of a contour plot in the CM system (such that CM is stationary).

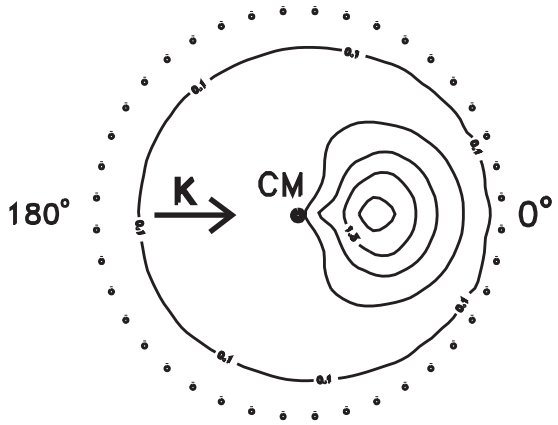

Contours represent lines of equal product flux as a function of KI velocity (*i.e.* flux as a function of scattering angle and KI speed).

Outer circle represents the maximum possible product velocity set by energy conservation (as obtained setting $E'_{\mathrm{t}} = \frac{1}{2}\mu' v'^2_{\mathrm{rel}} = E_{\mathrm{avl}}$, where E_{avl} is the total available energy to the products).

Observe forward scattering ($\theta \leq 90°$).

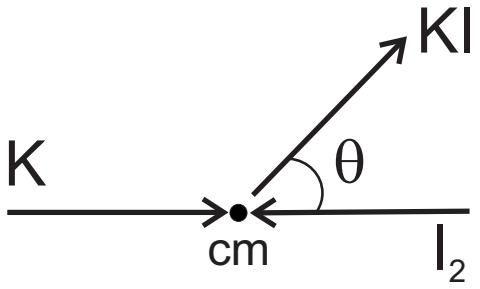

Harpoon mechanism

Observe:

- a very large reaction cross-section (like many other alkali + halogen reactions);
- forward scattered products;
- low energy release into translation (about 1/4 of the available energy). KI must be highly internally excited (see Polanyi's rules later).

Electron transfer (harpoon) takes place when

$$V_{\text{covalent}}(R_c) = V_{\text{ionic}}(R_c) \simeq 0\,,$$

i.e. when

$$I_K - EA_{I_2} = \frac{e^2}{4\pi\epsilon_0 R_c}\,.$$

$R_c \simeq 6$ Å in this case

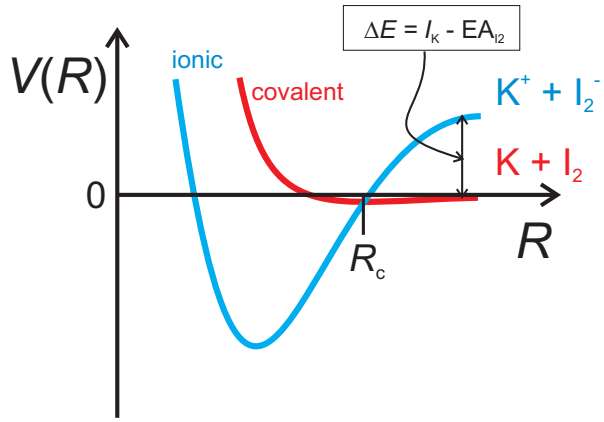

Estimate of the cross-section (assuming $P(b) = 1$)

$$\sigma = \int_0^{b_{max}=R_c} 2\pi b\,\mathrm{d}b \;=\; \pi R_c^2 \;\simeq\; 100\,\text{Å}^2$$

I_2^- formed with internuclear separation such that there is little repulsion between I and I^-.

K^+ carries off I^- in its original direction (forward scattering).

Rebound dynamics

$$K + CH_3I \longrightarrow KI + CH_3$$

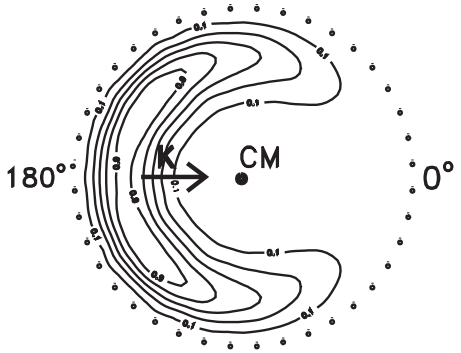

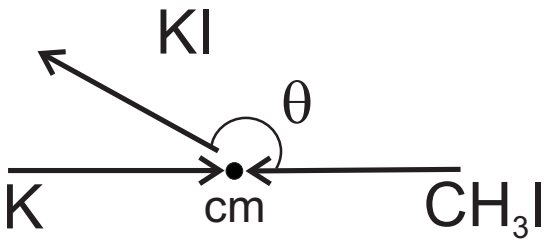

Observe

- This reaction has a *small cross-section*
- Dominated by *backward scattering* - consistent with reaction at small b
- Displays a high translational energy release into the products (see later).

This reaction is also a harpoon reaction, but EA_{CH_3I} is negative.

Therefore, the **curve crossing occurs at short range.**

$F + H_2(v = 0, j = 0, 1) \longrightarrow HF(v') + H$

HF product velocity-angle contour plot

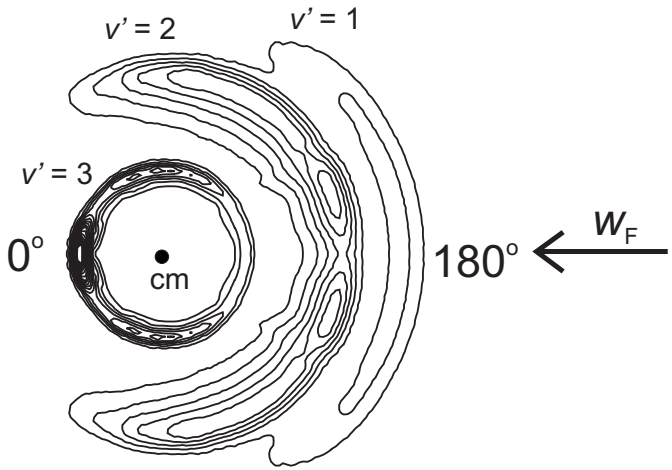

Product vibrational resolution

$v' = 1, 2$ *rebound dynamics*

$v' = 3$ *forward scattered*

The **HF vibrational population distribution** can be determined from the above contour plot by integrating over scattering angle.

Vibrational population inversion (see later)

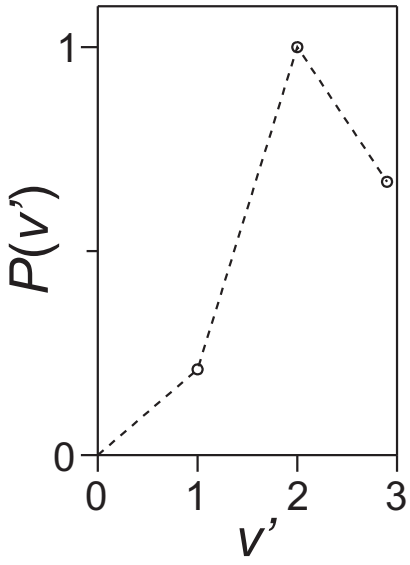

F + H_2 $\longrightarrow$ HF(v') + H - continued

Why was the structure observable?

1. High resolution apparatus (well collimated, *skimmed* molecular beams)

2. **Angular momentum conservation**

$$\boldsymbol{J}_{\text{tot}} = \boldsymbol{j}_{\text{H}_2} + \boldsymbol{L} = \boldsymbol{j}'_{\text{HF}} + \boldsymbol{L}' \, .$$

   (a) j_{H_2} small because of cooling of rotational degree of freedom in the molecular beam, and the large rotational B constant of H_2 (not many states populated even at 300 K).

   (b) Reaction has a small cross-section, preferentially occurs at small b, hence $|\boldsymbol{L}|$ $(= \mu v_{\text{rel}} b)$ also small (both b and μ small).

   (c) Therefore, little angular momentum available to the products. Note that $|\boldsymbol{L}'|$ $(= \mu' v'_{\text{rel}} b')$ also tends to be small because μ' is small.

3. HF vibrational levels well-separated in energy - large difference in product velocity.

$F + H_2 \longrightarrow HF(v') + H$ - continued

Why the forward peak?

This has been a controversial issue.

The clue is that the forward peak, although seen in classical calculations, is much weaker than observed quantum mechanically.

Unlike low v', reaction to generate $v' = 3$ arises from high impact parameter collisions, taking place close to the energetic threshold.

Reactions at these high $|\boldsymbol{L}|$ are not allowed classically because of the **centrifugal barrier**

$$V_{\text{eff}}(R) = V(R) + E_{\text{cent}}$$

$$E_{\text{cent}} = \frac{L^2}{2I} = \frac{(\mu v_{\text{rel}} b)^2}{2\mu R^2} = E_{\text{col}} \frac{b^2}{R^2}$$

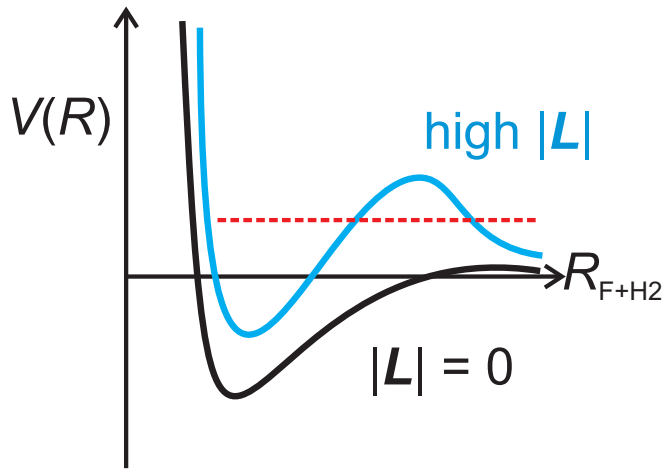

They are allowed by **quantum mechanical tunneling** through the centrifugal barrier.

$\mathbf{H + HD}(v = 0, j = 0) \longrightarrow \mathbf{H_2}(v', j') + \mathbf{D}$

Differential cross-section

State-of-the-art measurements using a laser ionization technique called *Rydberg-tagging* to detect the D atom products. Each ring in the pictures below corresponds to a fully resolved rovibrational quantum state of the H_2 coproduct (see later).

This reaction has a large barrier.

It displays **rebound dynamics** (backward scattering) at low collision energies.

However, the scattering becomes more sideways and forward as the collision energy is raised.

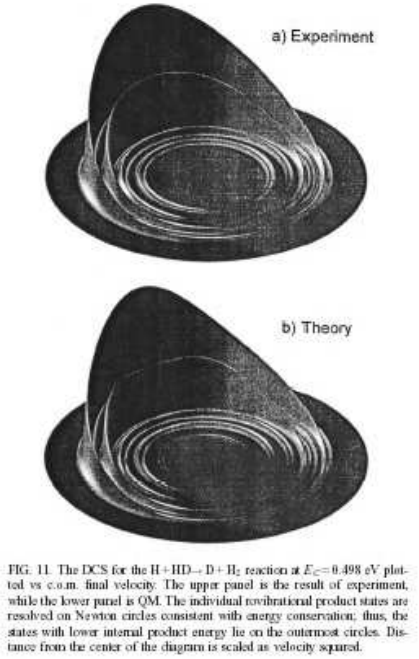

FIG. 11. The DCS for the H+HD→D+H_2 reaction at E_C=0.498 eV plotted vs c.o.m. final velocity. The upper panel is the result of experiment, while the lower panel is QM. The individual rovibrational product states are resolved on Newton circles consistent with energy conservation; thus, the states with lower internal product energy lie on the outermost circles. Distance from the center of the diagram is scaled as velocity squared.

$E_{\text{col}} \sim 0.5\,\text{eV}$
Rebound Dynamics

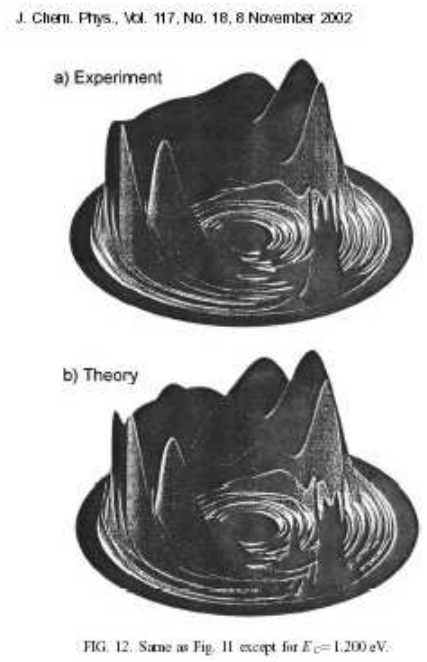

FIG. 12. Same as Fig. 11 except for E_C=1.200 eV.

$E_{\text{col}} \sim 1.2\,\text{eV}$
More forward scattering

X.M. Yang and coworkers *J. Chem. Phys.*, **117**, 8341, (2002).

Quantum mechanical scattering calculations

Importance of quantum mechanical tunneling in the F + H_2 reaction already discussed.

Quantum mechanical dynamical calculations are possible for light three-atom systems.

$$H + D_2 \longrightarrow HD(v', j') + D$$

$HD(v' = 3, j' = 2)$

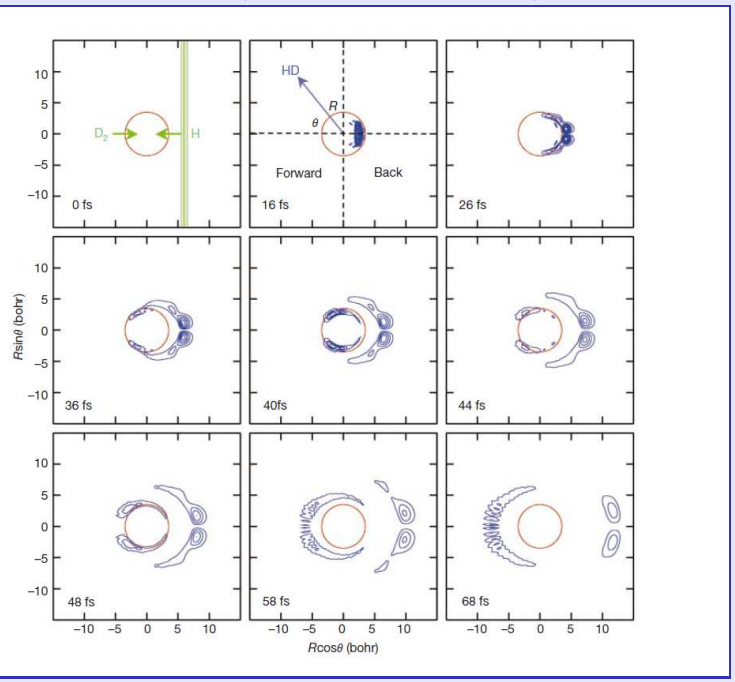

Provides important information about role of zero point energy, tunneling and other exotic QM effects.

S.C. Althorpe and coworkers *Nature* **416** 67 (2002)

Formation of complexes

Forward-backward symmetric angular distributions.

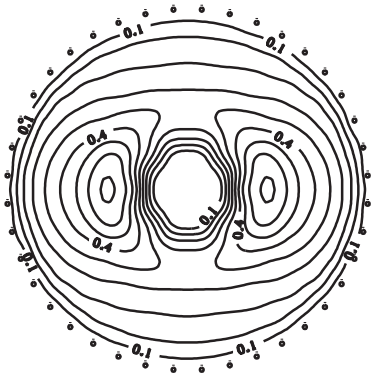

$$O + Br_2 \longrightarrow Br_2O^\star \longrightarrow BrO + Br$$

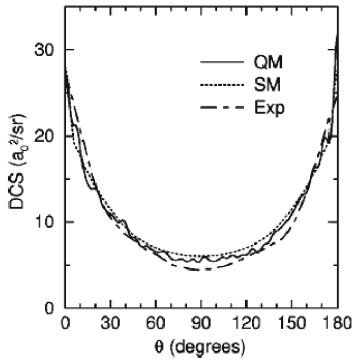

$$S(^1D) + H_2 \longrightarrow H_2S^\star \longrightarrow SH + H$$

Complex lifetime must be long compared to the rotational period.

Favoured by reactions on **attractive** potential energy surfaces (see later), which have large cross-sections and $b \gg 0$.

Scattering of products is uniform in the plane containing v_{rel} and b, but $\boldsymbol{L}$, which lies $\perp$ to this plane, can lie anywhere on the circle. Leads to

$$\frac{\mathrm{d}\sigma}{\mathrm{d}\omega} \sim \frac{1}{\sin\theta}$$

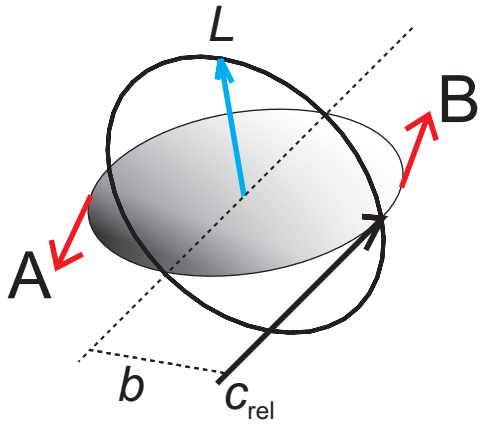

3. Controlling reagents and characterizing products

Effect of translational energy

How does reactant translational energy affect the rate of chemical reactions?

Velocity selection

Methods of velocity selection have been discussed in Professor Vallance's lectures. Velocity can be selected in a molecular beam through the use of mechanical choppers, control of the source pressure, and seeding gas.

Relative velocity (collision energy) can also be tuned by varying the molecular beam intersection angle

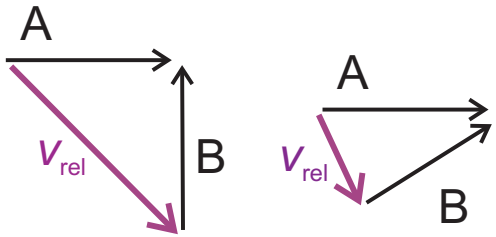

More recently, researchers have started to use the Stark or Zeeman effects to decelerate molecules.

As an alternative, one can use laser photolysis to produce velocity selected species. This can be useful for those species, such as H atoms, which are hard to generate in high concentrations in a molecular beam.

$$DI + h\nu \longrightarrow D + I$$

KE goes into light D atom (conservation of energy and momentum).

Vary KE of D by changing ν.

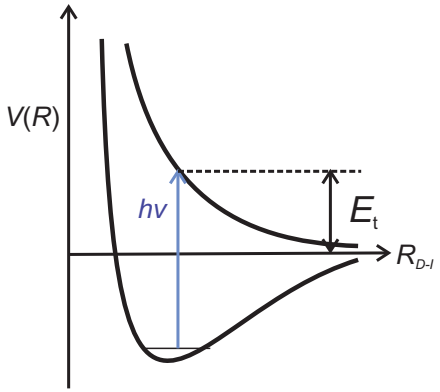

Excitation functions

Reactions with a barrier

For example

$$D + C_6H_{12} \longrightarrow HD + C_6H_{11}$$

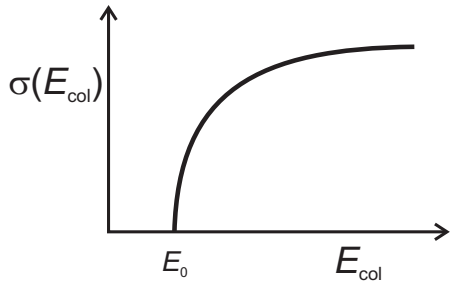

Shape of the *excitation function*, $\sigma(E_{\text{col}})$, is dictated by energy and angular momentum conservation, $|\boldsymbol{L}| = \mu v_{\text{rel}} b$.

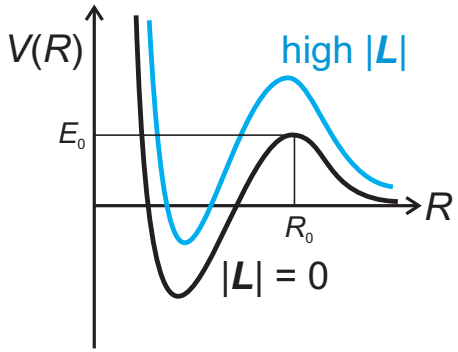

Just above E_0, collisions have enough energy to surmount the barrier on the PES, but they need to surmount the **centrifugal barrier**.

Only reactions at low b are therefore possible.

Consider an atom-atom collision (*e.g.*, hard spheres)

Factor the translational energy (which is the total energy when the atoms are far apart) into radial and centrifugal components.

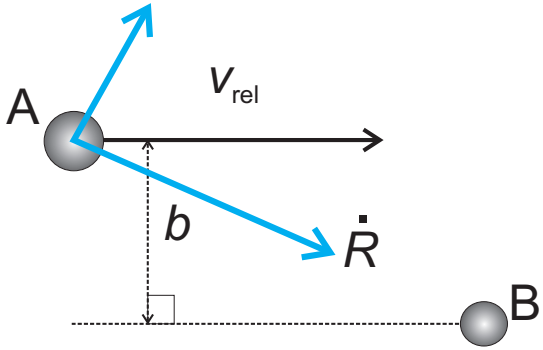

The classical Hamiltonian can be written:

$$H_{\text{class}} = E_{\text{tot}} = E_{\text{col}} \,,$$

Excitation functions - continued

and, therefore,

$$E_{\text{col}} = \frac{1}{2}\mu v_{\text{rel}}^2 = \frac{1}{2}\mu \dot{R}^2 + E_{\text{cent}} + V(R)\,,$$

where (see CV lectures)

$$E_{\text{cent}} = \frac{L^2}{2I} = E_{\text{col}}\frac{b^2}{R^2}\,.$$

Note that we can think of $E_{\text{cent}} + V(R)$ as the *effective potential*, $V_{\text{eff}}(R)$, on which collision takes place. Reaction can occur if the radial kinetic energy at the barrier is greater than zero, $\frac{1}{2}\mu\dot{R}^2 > 0$, *i.e.*

$$\frac{1}{2}\mu\dot{R}^2 = E_{\text{col}} - E_{\text{col}}\frac{b^2}{R_0^2} - V(R_0) > 0\,.$$

Given that $V(R_0)$ is simply the barrier height, E_0, this equation can be rearranged to give:

$$b_{\text{max}}^2 = R_0^2\left(1 - \frac{E_0}{E_{\text{col}}}\right)\,.$$

Assuming $P(b) = 1$ **for** $0 \leq b \leq b_{\text{max}}$, the cross-section can then be written

$$\sigma = \int_0^{b_{\text{max}}} P(b) 2\pi b \mathrm{d}b = \pi b_{\text{max}}^2 = \pi R_0^2\left(1 - \frac{E_0}{E_{\text{col}}}\right)\,.$$

This is the **line-of-centres model** for the reaction cross-section.

Excitation functions - continued

Reactions without a barrier

Many reactions, including insertion reactions such as $O(^1D) + H_2$, and ion-molecule reactions, do not possess barriers to reaction.

The model can be extended to such reactions, again treating the reactants as structureless atoms. We will encounter some examples in the problems class next term.

Example

The long range potential for an ion - induced dipole interaction can be approximated

$$V(R) = -\frac{C_4}{R^4}\,,$$

where C_4 is a constant.

Although there is no potential energy barrier, there is still a centrifugal barrier to surmount,

$$V_{\text{eff}}(R) = E_{\text{cent}} + V(R) = E_{\text{col}}\frac{b^2}{R^2} - \frac{C_4}{R^4}\,.$$

By setting $\mathrm{d}V_{\text{eff}}/\mathrm{d}R = 0$, the location of the centrifugal barrier is at

$$R_0 = \left(\frac{2C_4}{E_{\text{col}}b^2}\right)^{1/2}\,.$$

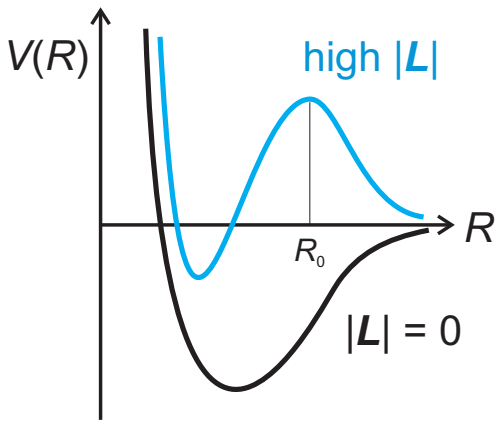

Excitation functions - continued

Now follow the same recipe as used above for reactions with a barrier:

- At the centrifugal barrier we require $\frac{1}{2}\mu\dot{R}^2 > 0$ for reaction to occur.
- Obtain an expression for b^2_{max}, from which the cross-section can be obtained (assuming $P(b) = 1$).

$$\sigma = \pi b^2_{\text{max}} = \pi \left(\frac{4C_4}{E_{\text{col}}}\right)^{1/2} \propto \frac{1}{v_{\text{rel}}}.$$

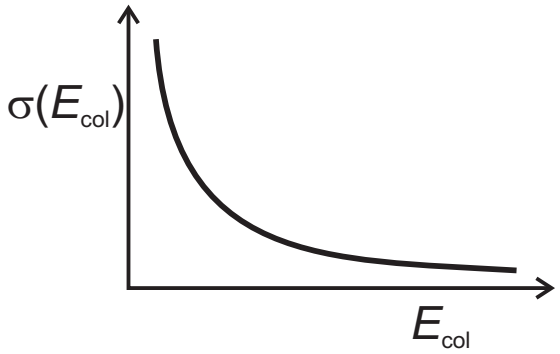

This is known as the **Langevin model**.

Rate constants for reactions without a barrier.

$$k(T) = \int_0^\infty v_{\text{rel}}\sigma(v_{\text{rel}})f(v_{\text{rel}})\mathrm{d}v_{\text{rel}}$$

Reactions between an ion and an induced-dipole are **temperature independent**.

The same treatment can be used to show that the rate constant between an ion and a dipole, or between two dipoles, *increases* as the temperature is *reduced*.

Such reactions play an important role in chemistry at low temperatures (such as found in space).

Effect of internal state excitation

As you have seen from Prof Vallance's lectures, internal states can also be selected by a variety of means, including *laser excitation*, or, for rotational states, using *inhomogeneous electric fields.*

Effect of vibrational excitation

How does reactant vibrational excitation affect the reaction cross section?

Example 1

$$\mathrm{K} + \mathrm{HCl}(v) \longrightarrow \mathrm{KCl} + \mathrm{H} \qquad \Delta H^{\ominus} = 4\,\mathrm{kJ\,mol^{-1}}$$

$\mathrm{HCl}(v = 1)$ has an energy of $34.5\,\mathrm{kJ\,mol^{-1}}$.

If this energy is localized into $\mathrm{HCl}(v = 1)$, the rate increases by $\times 100$.

If the same energy is put into relative translation, the rate only increases by $\times 10$.

Vibrational energy is $\sim$10 times more efficient at promoting reaction than translational energy.

Example 2

$$\mathrm{OH} + \mathrm{H_2}(v = 0, 1) \longrightarrow \mathrm{H_2O} + \mathrm{H}$$

Vibrational excitation of the $\mathrm{H_2}$ to $v = 1$ increases the rate constant by a factor of over 100 (*i.e.* $k_{v=1}(T) \gtrsim 100\, k_{v=0}(T)$).

Vibrational excitation of the 'spectator' OH reactant has very little effect on the reaction rate.

Selective utilization of vibrational excitation

Example 3

This example uses the **laser pump and probe** method.

$$\mathrm{HOD}(v=0) + h\nu \longrightarrow \mathrm{HOD}(v_i)$$

$$\mathrm{H} + \mathrm{HOD}(v_i) \longrightarrow \mathrm{OD/OH}(v', j') + \mathrm{H_2/HD}$$

H atoms were generated in a flow-system using a microwave discharge, while the OH/OD products were probed by laser induced fluorescence.

$\mathrm{H} + \mathrm{HOD}(\nu_{\mathrm{OH}} = 4) \longrightarrow \mathrm{OD} + \mathrm{H_2}$

Selectively breaks the OH bond

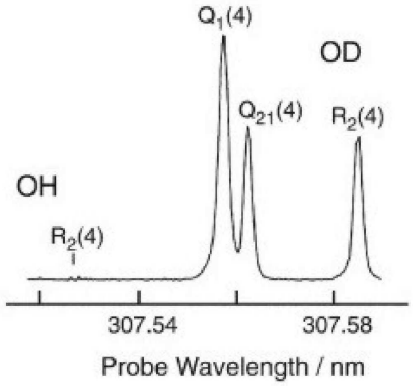

$\mathrm{H} + \mathrm{HOD}(\nu_{\mathrm{OD}} = 5) \longrightarrow \mathrm{OH} + \mathrm{HD}$

Selectively breaks the OD bond

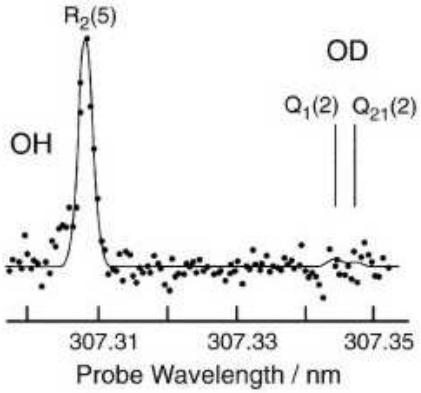

What about the effect of bending modes?

Is mode selectivity the exception or the rule (see IVR later)?

Potential energy surfaces (PESs) and Polanyi's Rules

To proceed further we need to think about the motion of nuclei over the potential energy surface.

Just consider *collinear collisions* for now (i.e. no rotation - see later).

$$\mathrm{A} + \mathrm{B}-\mathrm{C} \longrightarrow \mathrm{A}-\mathrm{B} + \mathrm{C}.$$

Consider the motion of the nuclei to be classical (*cf.* a ball rolling over a 3-D model of the PES).

The location of the barrier turns out to be critical

Early barrier

Kinetic energy effective in overcoming barrier (left)

Vibrational energy ineffective (right)

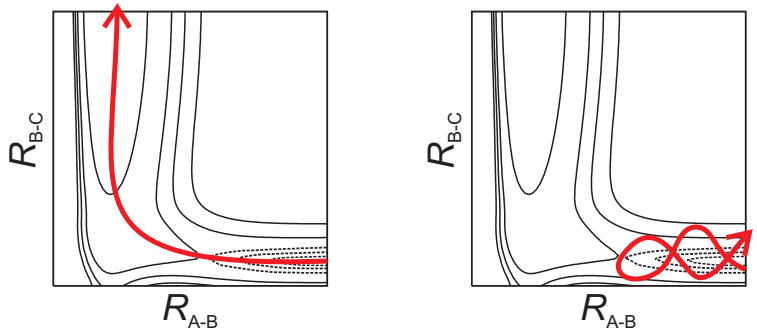

Late barrier

Vibrational energy effective in overcoming barrier (left)

Kinetic energy ineffective (right)

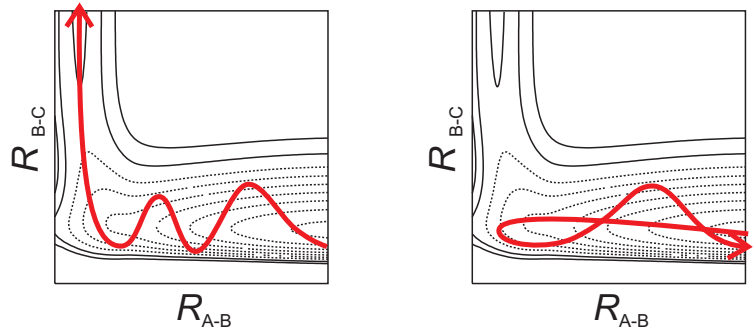

K + HCl(v) and OH + H_2(v) provide examples of reactions with late barriers.

Product state distributions and the disposal of energy

The previous examples focus on how translational and vibrational energy in the reactants can be used to initiate or promote reaction. However, what about the disposal of energy in the products of reaction?

Here we seek to measure the **populations** in different rovibrational quantum states of the products, since these provide information on the **state-resolved cross-sections**

$$P(v', j') = \frac{\sigma_{v',j'}}{\sigma},$$

provided that the total cross-section, σ, is known from other experiments.

How do we measure?

Molecular beams provide collision free environment, *i.e.* no scrambling of internal states by energy transfer, but internal state populations hard to measure in crossed beams. Generally need to use other methods, such as IR chemiluminescence, laser induced fluorescence (LIF), and resonantly enhanced multi-photon ionization (REMPI).

Example 1

$$O + CS \longrightarrow CO(v') + S$$

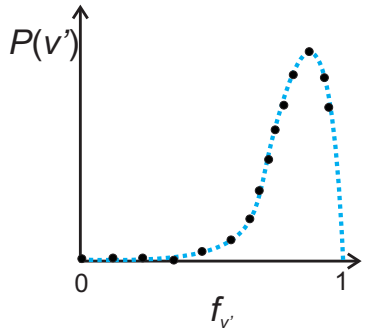

There is a **population inversion** in the CO product vibrational levels. These populations cannot be described by a Boltzmann distribution (*i.e.* not at thermal equilibrium).

Selective disposal of energy into vibration

Example 2

OH + D_2 $\longrightarrow$ HOD(ν_{bend}, ν_{OD}) + D

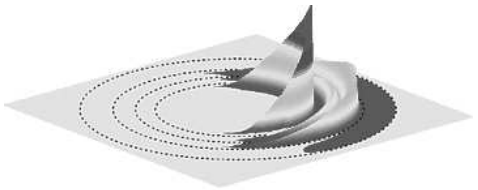

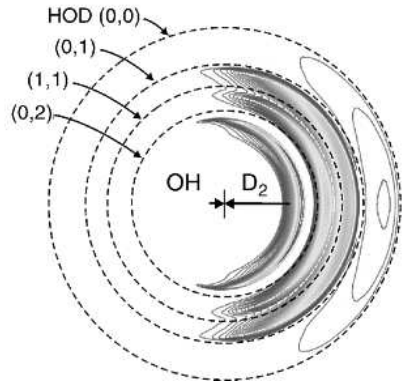

HOD product angular distributions

D atoms detected with high velocity resolution by Rydberg tagging in a molecular beam experiment (see CV lectures)

HOD product vibrational populations

Population inversion observed in the OD stretching mode (*cf.*, F + H_2)

No vibrational excitation observed in the OH stretching mode

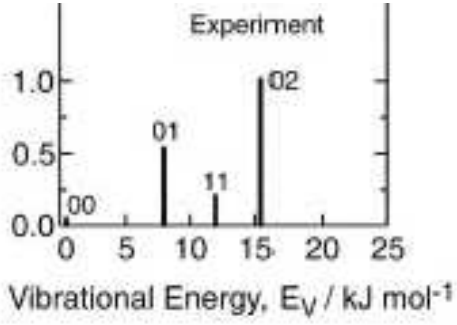

Crim and Smith, *Phys. Chem. Chem. Phys.*, **4**, 3543, (2002).

Microscopic reversibility and vibrational energy disposal

Each trajectory is invariant under time-reversal:

So to understand vibrational energy disposal, we can simply run the trajectories in reverse compared to the case of Polanyi's rules, using the principle of **microscopy reversibility**:

1. Early barrier - 'attractive release' of energy

Barrier occurs in the entrance channel

Exothermicity is released before A-B reaches equilibrium position

Preferential release of exothermicity into product vibration

(see O + CS and K + I_2)

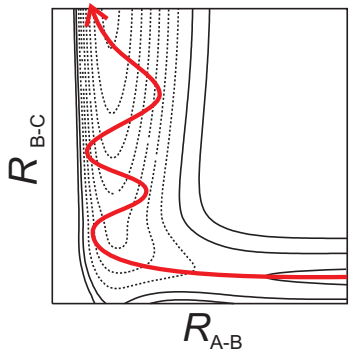

2. Late barrier - 'repulsive release' of energy

Barrier occurs in the exit channel

Exothermicity released as B-C bond extends

Preferential release of exothermicity into product translation

(see K + CH_3I)

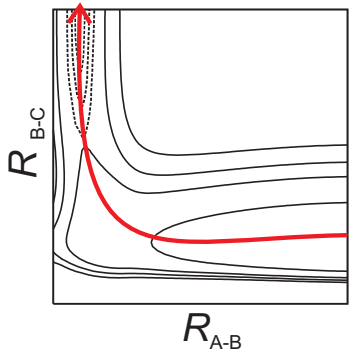

Often see a mixture of the two types of trajectories (leading to a mixed release of energy).

Role of kinematics

As you have seen previously, to preserve the model of a ball rolling a 3-D model of the PES need to take into account masses of reactants and products. Instead of plotting the PES with 90° coordinates, the coordinates should be **skewed** at an angle β, defined for an A + BC reaction as

$$\cos^2\beta = \frac{m_A m_C}{m_{AB} m_{BC}}.$$

So for a reaction

$$\mathcal{L} + \mathcal{H}\mathcal{H}' \longrightarrow \mathcal{L}\mathcal{H} + \mathcal{H}' \qquad \beta \sim 90^\circ$$

while for

$$\mathcal{H} + \mathcal{L}\mathcal{H}' \longrightarrow \mathcal{H}\mathcal{L} + \mathcal{H}' \qquad \beta \ll 90^\circ$$

where $\mathcal{H}$ = heavy atom, $\mathcal{L}$ = light atom.

For example, for

$$Cl + HI \longrightarrow HCl + I \qquad \beta = 10.7^\circ$$

One finds 70% of the available energy in this reaction is channeled into vibrational excitation, in spite of the barrier being late.

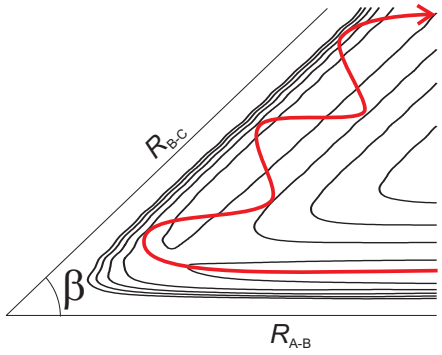

Polanyi's 'rules' (and the reverse of them) only apply to reactions involving light attacking or departing atoms.

Angular momentum conservation

Again focus on A + BC reaction, and think about role of masses in context of angular momentum conservation.

Recall

$$\boldsymbol{J}_{\text{tot}} = \boldsymbol{j}_{\text{BC}} + \boldsymbol{L} = \boldsymbol{j}'_{\text{AB}} + \boldsymbol{L}' \,.$$

Take a reaction

$$\mathcal{H} \;+\; \mathcal{H}'\mathcal{L} \;\longrightarrow\; \mathcal{H}\mathcal{H}' \;+\; \mathcal{L}\,,$$

for which $\beta \sim 90°$, the mass combination favours $\boldsymbol{L} \gg \boldsymbol{j}_{\text{BC}}$, while for the products $\boldsymbol{j}'_{\text{AB}} \gg \boldsymbol{L}'$. Thus we can write

$$\boxed{\boldsymbol{L} \;\longrightarrow \boldsymbol{j}'_{\text{AB}}\,,}$$

i.e. there is a **propensity for the reactant orbital angular momentum to be channeled into product rotational angular momentum** (see later).

Similarly for the mass combination

$$\mathcal{H} \;+\; \mathcal{L}\mathcal{H}' \;\longrightarrow\; \mathcal{H}\mathcal{L} \;+\; \mathcal{H}'\,,$$

for which $\beta \ll 90°$, angular momentum conservation often reduces to

$$\boxed{\boldsymbol{L} \;\longrightarrow \boldsymbol{L}'\,,}$$

i.e. there is a **propensity for conservation of orbital angular momentum**.

Direct versus indirect reactions

So far we have mainly considered trajectories for **direct** reactions.

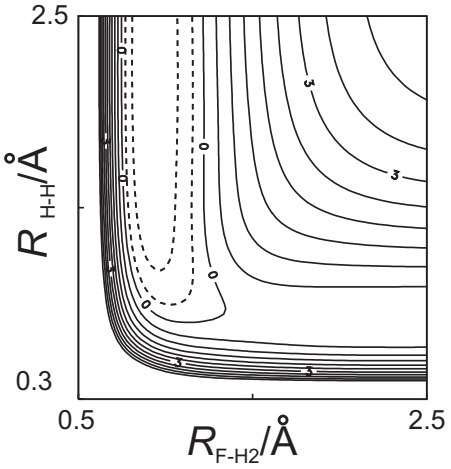

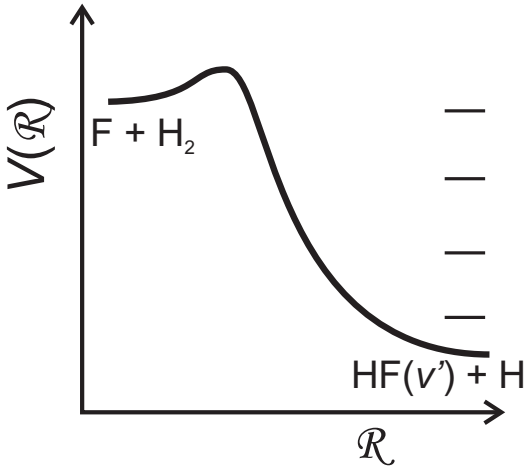

What about trajectories on a PES with deep well, which lead to the formation of an intermediate **complex**?

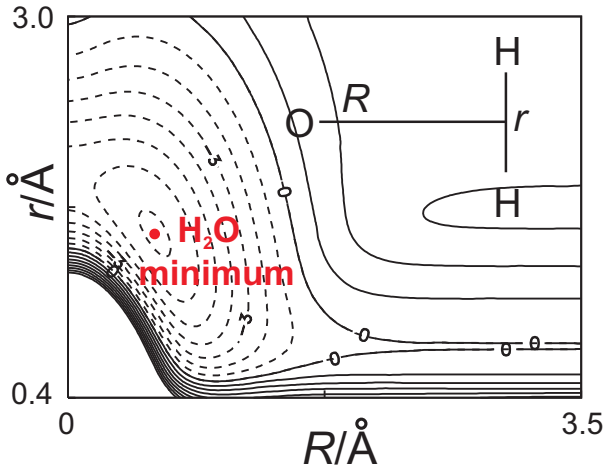

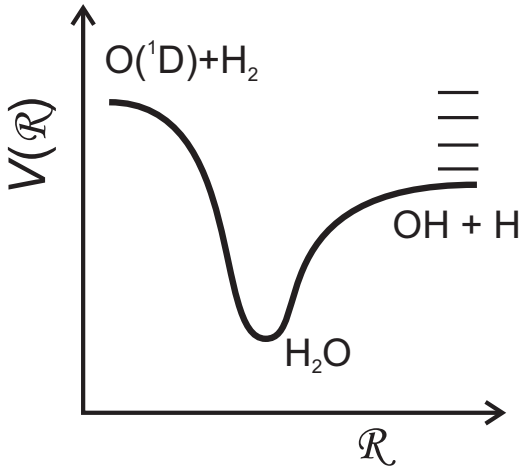

Example: Insertion reactions

$$\textbf{Pump} \quad O_3 + h\nu \longrightarrow O(^1D) + O_2$$

$$\textbf{Probe} \quad O(^1D) + CH_4 \longrightarrow OH(v', j') + CH_3$$

$OH(v', j')$ probed using laser induced fluorescence.

Use pulsed lasers (of 10^{-8} s pulse-length) for both pump and probe steps.

Employ low pressures and short pump-probe time-delay to avoid collisional energy transfer, which would lead to scrambling of the energy disposal in OH.

Observe significant population in all energetically accessible rovibrational states.

This **insertion reaction** forms highly rovibrationally excited $CH_3OH^\star$ which lives for a period of short time ($\leq$ a few picoseconds) before reaction occurs.

$$O(^1D) + CH_4 \longrightarrow CH_3OH^\star \longrightarrow OH(v', j') + CH_3$$

Statistical products state distributions

Trajectories can get trapped in the well.

If the complex survives for many **vibrational periods** (~ 100 fs) the vibrational energy can become completely randomized.

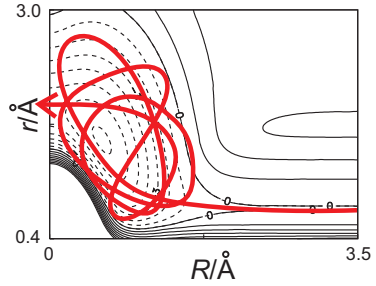

This randomization process is known as **intramolecular vibrational redistribution, (IVR)**.

Under these conditions the product quantum states may also be randomly or **statistically** populated (*i.e.* every 'state' has an equal probability of being populated).

We can estimate the populations most easily in this case using the **prior distribution**. Ignore angular momentum conservation.

Probability of finding product diatom in state j' is $\propto (2j'+1)$

Probability of finding translational energy, $E'_{\text{col}} (= \frac{1}{2}\mu' v'^2_{\text{rel}})$ *is* $\propto E'^{\frac{1}{2}}_{\text{col}}$

Therefore

$P(v', j') \propto (2j'+1)\,[E_{\text{avl}} - E'_{\text{v}} - E'_{\text{r}}]^{\frac{1}{2}}$,

where E_{avl} is the total energy available to the products.

$$O(^1D) + H_2 \longrightarrow OH(v', j') + H$$

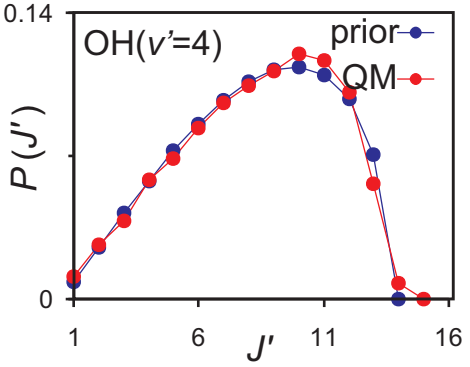

4. Probing transition states

Probing the steric factor

As you have seen, it is possible to select the rotational quantum state of a symmetric top molecule using a **hexapole electric field**. The **orientation** of quantum state-selected molecule in molecular beams can then controlled using a **weak static electric field**.

This then enables a **direct determination of the steric factor, p:**

$$Rb + CH_3I \longrightarrow RbI + CH_3$$

Look for RbI in the backward scattered direction - only see signal when I end of CH_3I is pointing towards the Rb beam.

Measurement of the reaction probability as a function of angle of attach, γ

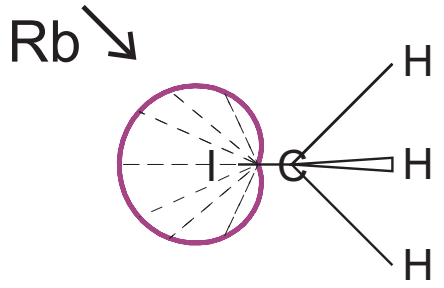

For this reaction the barrier height depends on the **angle of attack, γ**. This can be explained using an angle dependent line-of-centres model (see Levine and Bernstein).

Not all reactions display strong steric effects, *e.g.*, reactions which proceed on PESs without barriers tend not to.

Measurement of the opacity function

Is it possible to determine the opacity function, $P(b)$, directly experimentally? This is difficult to do, because collisions inherently average over the impact parameter.

One solution to this problem is the study kinematically constrained reactions. Let us **look at angular momentum constraints once more:**

$$\mathrm{Ba} \;+\; \mathrm{HI} \;\longrightarrow\; \mathrm{BaI}(v', j') \;+\; \mathrm{H}$$

Example of reaction with light departing atom for which $\boldsymbol{L} \rightarrow \boldsymbol{j'}$

Using LIF, measure the population distribution, $P(j')$, over product rotational states j' for each v' state at a well defined v_{rel}.

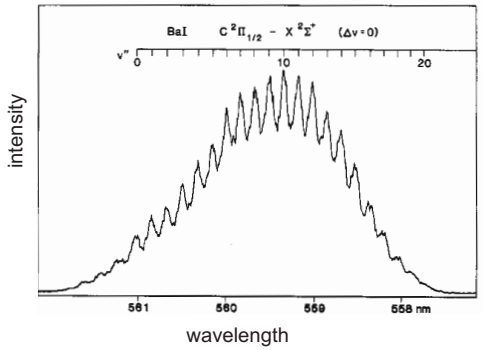

R.N. Zare and coworkers, *J. Chem. Phys.* **85** 856 (1986)

Due to angular momentum conservation contraints

$$P(j') \equiv P(L)$$

But

$$|\boldsymbol{L}| = \mu v_{\mathrm{rel}} b = \hbar\sqrt{L(L+1)} \simeq \hbar(L+1/2)$$

So $P(L)$ transforms directly into $P(b)$

The experimentally determine opacity functions, $P(b)$, reveal that low impact parameter collisions lead to generation of the highest BaI vibrational excitation.

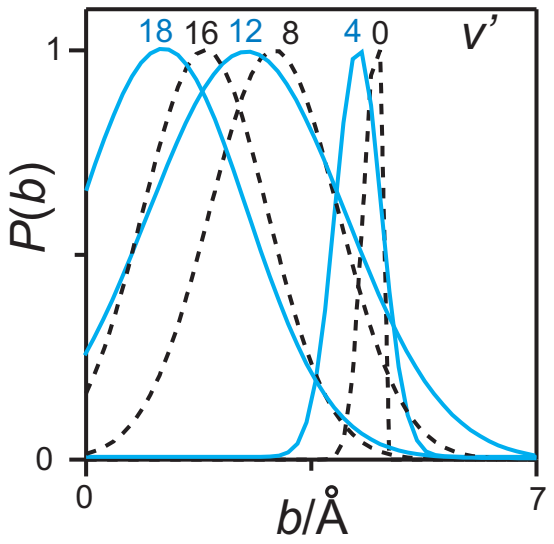

Angular momentum polarization

Measurement of the polarization of the angular momentum after a collision also provides a means of unpealing the averaging over impact parameter, b.

Angular momentum is a vector. **In what direction does j' point after reaction?**

Again focus on A + BC reactions.

$$H + D_2 \longrightarrow HD(j') + D$$

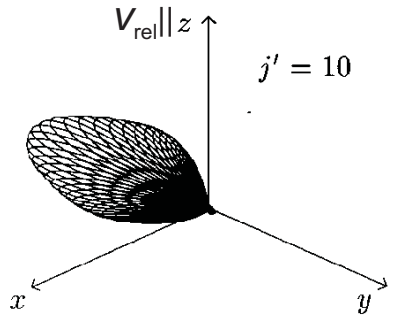

The zx-plane (the 'scattering' plane) contains both v_{rel} and v'_{rel}. Data imply that this **direct reaction is highly coplanar**.

$$O(^1D) + HD \longrightarrow OH(j') + D$$

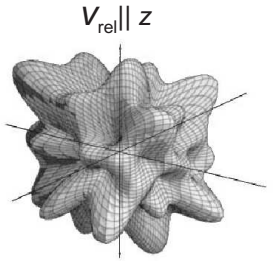

j'=10

This **insertion reaction behaves very differently - it is highly non-coplanar**.

These are calculated data, but angular momentum polarization can be measured experimentally using polarized light.

Aoiz and de Miranda and coworkers, *J. Chem. Phys.* **114**, 8329, (2001); **111**, 5368, (1999).

Half-collisions and controlling the impact parameter

A further way to control the collision geometry is to initiate reaction from within a **van der waals complex**, in this case IH—OCO, made by co-expansion of HI and CO_2 in a molecular beam.

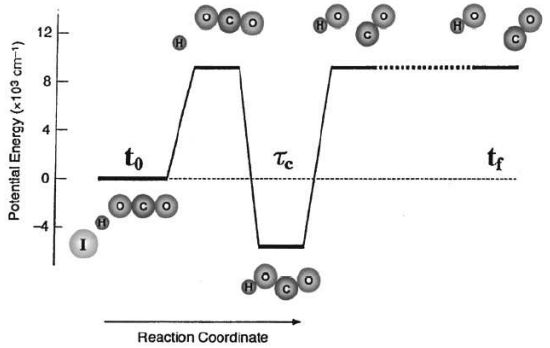

Start the H + CO_2 reaction by laser flash photolysis of HI (bound in the complex). Monitor OH production by LIF as a function of time.

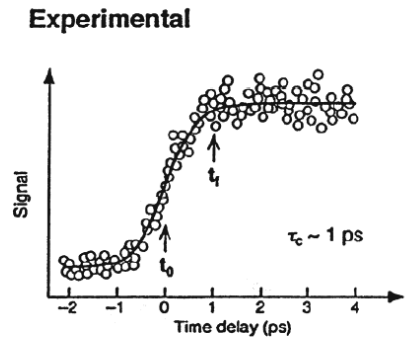

Reaction proceeds *via* an HOCO complex. It survives for about 1 ps. The results can be modeled using a statistical model of reaction rates.

A.H. Zewail, *J. Phys. Chem. A* **104**, 5660, (2000)

Femtochemistry

The following example of a **'half collision'** study involves the photodissociation of NaI.

The dissociation process involves a mechanism similar to a *harpoon reaction*, but studied in a half collision. The experiment illustrates one of the first to probe the transition state of a reaction in real time.

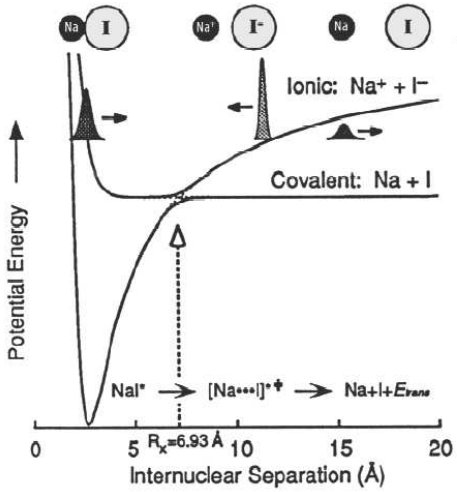

Dissociation of NaI* to Na + I products arises from a crossing between the ionic and covalent potential energy curves.

The time-resolved Na product and NaI* 'activated complex' signals on the right show oscillations which reflect the vibrational oscillations in the NaI* molecule. Dissociation occurs every time the 'wavepacket' of NaI* passes the crossing region between the ionic and covalent curves.

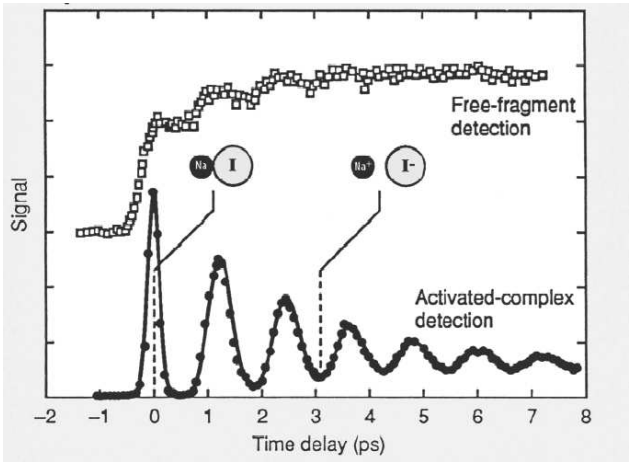

A.H. Zewail, *J. Phys. Chem. A* **104**, 5660, (2000)

Observing the Transition State region.

This experiment provides one of the first examples of the spectroscopic probing of the transition state region of a chemical reaction, this time $F + H_2$.

Photoelectron spectroscopy of F–p-H_2^-

Measure the kinetic energies of the ejected photoelectrons

$$[F - pH_2]^- \xrightarrow{h\nu} [F - pH_2]^{\ddagger} + e^-$$

The neutral products are produced in geometries very close to those of the transition state for the reaction $F + pH_2 \rightarrow HF + H$.

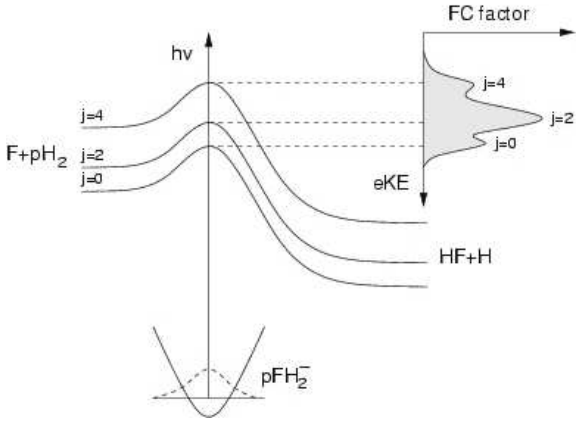

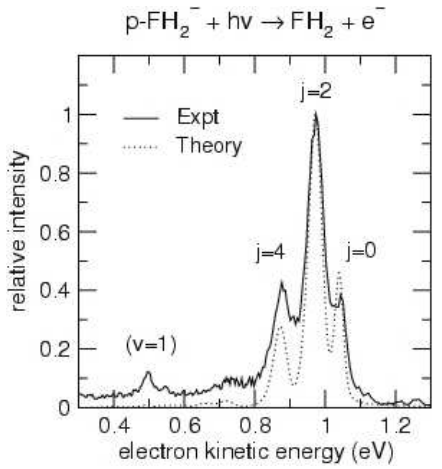

The spectrum suggests that the transition state is bent

Manolopoulos and Neumark and coworkers, *Science*, **262**, 1852, (1993).